

Nebulin as a Length Regulator of Thin Filaments of Vertebrate Skeletal Muscles: Correlation of Thin Filament Length, Nebulin Size, and Epitope Profile

Marlena Kruger, John Wright, and Kuan Wang

Clayton Foundation Biochemical Institute, Department of Chemistry and Biochemistry, Cell Research Institute, University of Texas at Austin, Austin, Texas 78712

Abstract. Nebulin, a family of giant proteins with size-variants from 600 to 900 kD in various skeletal muscles, have been proposed to constitute a set of inextensible filaments anchored at the Z line (Wang, K., and J. Wright. 1988. *J. Cell Biol.* 107:2199–2212). This newly discovered filament of the skeletal muscle sarcomere is an attractive candidate for a length-regulating template of thin filaments. To evaluate this hypothesis, we address the question of coextensiveness of nebulin and the thin filament by searching for a correlation between the size of nebulin variants and the length distribution of the thin filaments in several skeletal muscles. A positive linear correlation indeed exists for a group of six skeletal muscles that display narrow thin filament length distributions.

To examine the molecular and architectural differences of nebulin size-variants, we carried out immunoelectron microscopic studies to map out epitope profiles of nebulin variants in these muscles. For this purpose, a panel of mAbs to distinct nebulin epitopes was produced against rabbit nebulin purified by an im-

proved protocol. Epitope profiles of nebulin variants in three skeletal muscles revealed that (a) nebulin is inextensible since nebulin epitopes maintain a fixed distance to the Z line irrespective of the degree of sarcomere stretch; (b) a single nebulin polypeptide spans a minimal distance of 0.9 μm from the Z line; (c) nebulin contains repeating epitopes that are spaced at 40 nm or its multiples; (d) nebulin repeats coincide with thin filament periodicity; (e) nebulin variants differ mainly at either or both ends; and (f) nebulin remains in the sarcomere in actin-free sarcomeres produced by gelsolin treatment. Together, these data suggest that nebulin is an inextensible full-length molecular filament that is coextensive with thin filaments in skeletal muscles.

We propose that nebulin acts as a length-regulating template that determines thin filament length by matching its large number of 40-nm repeating domains with an equal number of helical repeats of the actin filaments.

THE lengths of thick and thin filaments in the sarcomeres of most vertebrate skeletal muscles are precisely regulated and are important structural parameters in understanding muscle contraction. The mechanisms of such precise length regulation have yet to be elucidated. It is clear from recent studies that although self-assembly of myosin, actin and the contribution of accessory proteins, such as C-protein and tropomyosin, are of major importance in the understanding of the assembly and morphology of myofilaments, these factors by themselves are not sufficient to consistently produce a population of filaments with uniform and defined length (for recent reviews, see 2, 14, 17). The recent discovery of titin and nebulin, two giant proteins which constitute a filamentous matrix that coexists with thick and thin filaments, has led to the hypothesis that these proteins may

serve as length regulating templates or scaffolds for thick and thin filaments of skeletal muscles (for reviews, see 10, 21, 22). The $\sim 1\text{-}\mu\text{m}$ -long titin strands span half a sarcomere and connect thick filaments, through structural association along their length, to the Z line. Titin also plays a pivotal role in organizing or regulating sarcomere assembly and may regulate the length of thick filaments (see reviews, 10, 21, 22).

Nebulin, a family of giant proteins with size variants from 600 to 900 kD in various skeletal muscles, has been proposed as a candidate for a length regulating template of thin filaments in skeletal muscles (23). This idea originated from antibody localization studies showing that nebulin epitopes maintain a fixed distance to the Z line irrespective of the degree of stretch of the sarcomere, as if nebulin constitutes a set of inextensible molecular filaments anchored at the Z line (23). The observation that nebulin and actin filaments act in concert when sarcomeres are subjected to overstretch further supports a structural association between the two filaments

A portion of this work has been presented at the 34th Biophysical Society meeting (Kruger, M., J. Wright, and K. Wang. 1990. *Biophys. J.* 57:554a).

(11). It was not possible, however, to conclude from such morphological studies the molecular interactions that might underlie such an association.

Since this template hypothesis of nebulin has significant structural and functional implications in the understanding of the physiological roles of thin filaments, we have initiated a series of experiments to systematically evaluate this proposal. Specifically, our laboratory is addressing whether nebulin possesses the following two important attributes of a molecular template for myofilaments: first, does it have multiple binding sites for actin and/or regulatory proteins such as tropomyosin and troponin? Second, are nebulin and thin filaments coextensive in the sarcomere?

Recent studies from our laboratory have now provided direct biochemical evidence that nebulin does indeed interact with actin filaments. In particular, molecular cloning and expression studies of the repetitive sequence motifs of human nebulin indicate that nebulin is a giant actin binding protein with multiple actin binding sites along its length (7).

In this paper we address the second question, i.e., the coextensiveness of nebulin and thin filaments. A promising approach was suggested by the observation that nebulins fall into several size classes, depending on the species and muscle tissues (5, 9, 23). The presence of nebulin size variants in these muscles thus offered an opportunity to search for a correlation between nebulin size and thin filament length as a manifestation of coextensiveness. Additionally, we addressed the following questions that are relevant to the template hypothesis. First, is nebulin inextensible and anchored at the Z line as we proposed (23), or does it exhibit elastic stretch dependence, as suggested by the data of Furst et al. (4)? Second, what are the molecular and architectural differences of nebulin size variants? For these purposes, we prepared a panel of distinct monoclonal antibodies and carried out immunoelectron microscopic studies to map out epitope profiles of nebulin variants in a group of selected skeletal muscles. The results presented in this paper support the inextensible nature of nebulin in intact sarcomeres, as we have proposed previously (23). Epitope profiles of nebulin variants revealed the presence of structural repeats of 40 nm or its multiples along certain regions of the nebulin molecule. The matching of nebulin molecular repeat and thin filament half-helical periodicity suggests a basis of molecular association and length regulation between the nebulin template and actin filaments.

Materials and Methods

Nebulin Size Variants

Size variants of nebulin in skeletal muscle tissues from human quadriceps (HQ),¹ snake skeletal muscle (SN), rabbit longissimus dorsi (LD), rabbit psoas (PS), chicken posterior latissimus dorsi (CPLD), and chicken pectoralis (CP) were identified by electrophoresis and Western blots essentially as described (16, 23). For molecular weight calibration, projectin from indirect flight muscle of *Lethocerus* (6) and human apolipoprotein B were coelectrophoresed as standards.

1. *Abbreviations used in this paper:* CP, chicken pectoralis; CPLD, chicken posterior latissimus dorsi; HQ, human quadriceps; LD, rabbit longissimus dorsi; PS, rabbit psoas; SN, snake skeletal muscle.

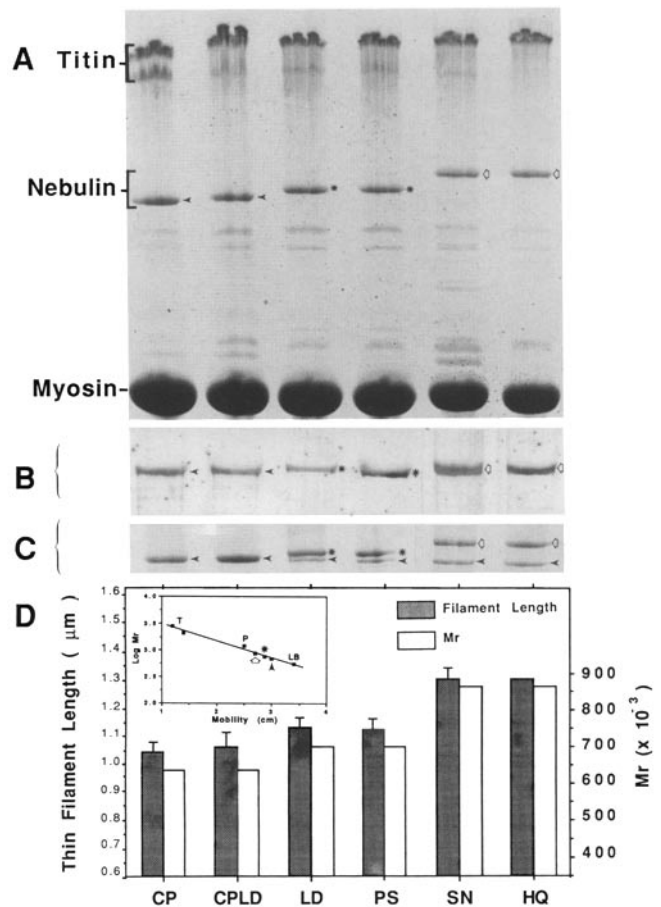


Figure 1. Nebulin size variants and thin filament lengths of skeletal muscles. Six muscle tissues were snap frozen, pulverized in liquid nitrogen, solubilized in hot SDS solution, and analyzed on a 2–12% gradient polyacrylamide gel (A, only proteins larger than myosin heavy chain are shown). To identify nebulin variants, Western blots were done with polyclonal anti-rabbit nebulin antiserum (B, only nebulin variants are shown). To reveal small mobility differences, an aliquot of chicken pectoralis (CP) gel sample was added to each muscle sample as an internal standard (C, only nebulin variants are shown). Note that nebulin increases in size in the following order: chicken pectoralis (CP), chicken posterior latissimus dorsi (CPLD) < rabbit longissimus dorsi (LD), rabbit psoas (PS) < snake skeletal (SN), human quadriceps (HQ). The apparent molecular weight of each nebulin variant was estimated by a plot of log M_r versus gel mobility, with titin (T), insect projectin (P), and human apolipoprotein B (LB) as calibration standards (D, inset). The average length of thin filaments of each of the six skeletal muscles (the bar represents the standard deviation, from Fig. 2 and reference 29 for HQ) was compared to the estimated size of nebulin variant in the bar chart (bottom). Note that muscles with longer thin filaments also express larger nebulin.

Purification of Nebulin

Rabbit skeletal muscle nebulin was purified essentially as described (23) except with an additional anion-exchange chromatography final step (Accell QMA; Millipore Corp., Bedford, MA) designed to remove trace amounts of titin fragments from nebulin. Briefly, nebulin fractions from the S-500 gel filtration column were pooled and concentrated fourfold by an ultrafiltration membrane (YMI00; Amicon Corp., Danvers, MA), followed by dialysis against 5 M urea; 10 mM Tris-Cl; 5 mM EGTA, pH 8.0. The dialyzed sample (10 ml) was applied to an Accell QMA column (22 ml), equilibrated in the same urea buffer, and then eluted with a linear gradient of 0–2.0 M NaCl in the urea buffer (total 80 ml). Nebulin was eluted be-

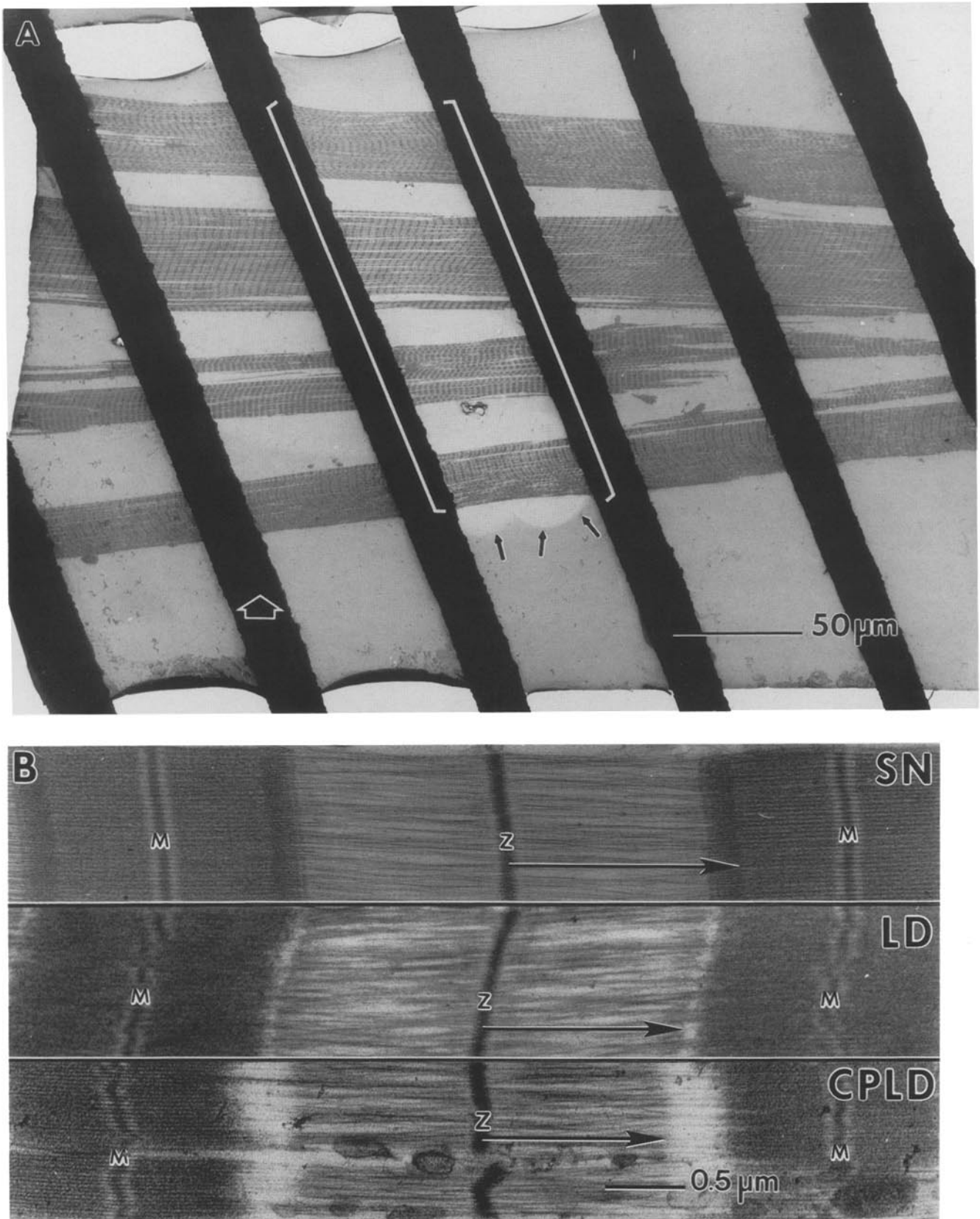


Figure 2. Parallel processing of split-fibers for thin filament length measurement. (A) A group of four split fibers was mounted in parallel on an EFA parallel bar grid, fixed, embedded, and sectioned. This low magnification survey electron micrograph illustrates the degree of alignment of fibers and the direction of sectioning (*open arrow*). The areas of observation and photography are indicated by the brackets. Small arrows point to the low density circles caused by electron irradiation. (B) Thin filament length was measured from the center of each Z-line to the border of the H zone (SN) or to the edge of the I-segment in nonoverlap sarcomeres (LD, CPLD).

tween 0.15 M and 0.30 M NaCl, followed by a large A280 nm peak containing SDS.

mAbs

Anti-Rabbit Nebulin. For immunization, nebulin purified by Accell QMA was dialyzed at room temperature into buffer F (40 mM Tris-acetate; 20 mM sodium acetate; 2 mM EDTA; 0.1% SDS; 0.2 mM DTT, pH 7.4). Before injection, nebulin was diluted fourfold to 0.2 mg/ml in PBS (10 mM KH_2PO_4 ; 150 mM NaCl, pH 7.4) and spun for 10 min in a microfuge to remove minor amounts of aggregate. Balb/c mice were immunized intrasplenically with 10 μg nebulin/mouse followed by weekly intravenous boosts with 10 μg nebulin/mouse for 6 wk. Antibody titer was detected by Western blotting at the fourth week. Two mice with the highest titer were selected and boosted intravenously with 30 μg nebulin/mouse 3 d before fusion. Spleen cells were mixed and then fused with nonsecreting SP2/0 mouse myeloma cells. Supernatants were screened and selected by Western blotting of total rabbit myofibrillar proteins as well as by immunofluorescent staining of glycerinated rabbit psoas myofibrils. Positive colonies were subcloned by limiting dilution. 18 stable clones were selected after three subclonings (for a total of 56 d). Secreted antibodies in the supernatants were typed by an mAb-based mouse immunoglobulin isotyping kit (PharMingen; San Diego, CA). Ascites fluids were elicited in female Balb/c mice primed with pristane. Immunoglobulins were purified from ascites fluids by protein A-affinity column (Affigel Protein A MAPS II kit; Bio-Rad Laboratories, Richmond CA).

Anti-Chicken Nebulin. NB2, as described by Furst et al. (4), was purchased from Sigma Chemical Co. (St. Louis, MO) as ascites fluid.

Western Blots

Rabbit myofibrillar proteins were first electrophoresed on 2–12% gradient SDS gels (16) and then transferred to nitrocellulose (NC) paper with a semidry transfer unit (Bio-Rad Laboratories) at 150 mA/gel in Kyhse-Anderson buffer (8). The blots were blocked either directly (blocking buffer: 0.1% BSA, 0.2% gelatin, 0.1% Tween-20 in PBS) for 90 min or after boiling for 30 min in H_2O to enhance sensitivity of some antibodies (18). Strips of blot were treated with mAbs overnight at room temperature, washed with PBS plus Tween-20 for 45 min and then treated with rabbit anti-mouse gold conjugates for 3 h. Visualization of gold beads by silver enhancement was done according to the manufacturer's protocol (Bio-Rad Laboratories).

Nebulin Epitope Profiles

Epitope profiles were determined by immunoelectron microscopy of mechanically split fibers essentially as described by Wang and Wright (23). The following modifications were made to ensure precise quantitative comparison. Briefly, a set of four split fibers was mounted in parallel on a single-slot gold grid (model GS2 \times 1; Polysciences, Inc., Warrington, PA). To accomplish this delicate procedure, four parallel cuts (0.4 mm long, 0.08 mm apart) were first made with a finely pointed scalpel blade (#11; Surgical Instruments of America, Cliffside Park, NJ) on each of the opposite sides of the gold grid such that four split fibers could be wedged into these cuts in parallel. Care was taken to keep the gold grid flat throughout the mounting and subsequent processing to allow all four fibers to be sectioned, stained, and photographed simultaneously as a set.

Grids with split fibers were transferred to freshly prepared formaldehyde/PBS fixative (3.7% paraformaldehyde, 2.7 mM KCl, 1.5 mM KH_2PO_4 , 130 mM NaCl, 8 mM Na_2HPO_4 , pH 7.2) for 10 min at 0°C and washed once in PBS for 10 min. The grid-mounted split fibers were blocked in 1% BSA/PBS for 15 min and then incubated with each of the primary antibody solutions (N46, N62: 50 $\mu\text{g}/\text{ml}$; NB2: 200 $\mu\text{g}/\text{ml}$ or 1:200 dilution of ascites in 1% BSA/PBS) in a microtiter plate (Terasaki Microwell plate; Nunc 163118, Southland Cryogenics, Carrollton, TX) for 15 h at 4°C and washed in five changes of BSA/PBS over 30 min at 4°C. Secondary antibody (affinity purified rabbit anti-mouse total immunoglobulins at 50–100 $\mu\text{g}/\text{ml}$ in PBS/BSA) was applied for 6 h at 4°C and washed with five changes of PBS/BSA over 30 min at 4°C. The fibers were then labeled by protein A-colloidal gold conjugate (3–5-nm-diam A_{512} =0.1) for 15 h at 4°C and washed in two changes of PBS/BSA over 15 min and five changes of PBS over 30 min.

Electron Microscopy

Grids with split fibers were transferred to BEEM capsules (size 00; Poly-

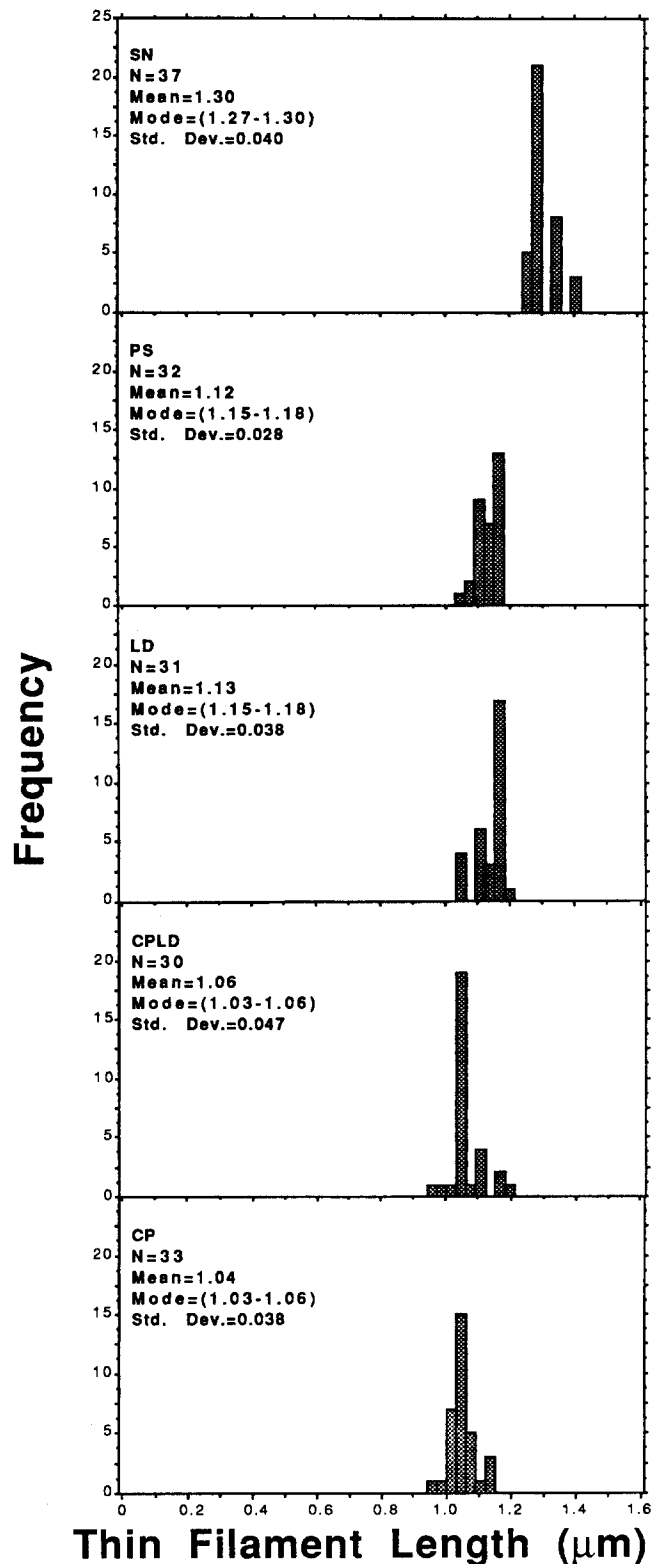


Figure 3. Thin filament length distribution. The distribution profiles of thin filament length of five muscles are presented as frequency plots. Note that the mean length of thin filaments increases in the following order: CP, CPLD < LD, PS < SN.

sciences, Inc.) fixed in 2% glutaraldehyde, 0.05 M Na cacodylate, pH 7.4 at 4°C for 40 min, washed in 0.05 M Na cacodylate, pH 7.4, and treated with 1% osmium tetroxide, 0.05 M Na cacodylate for 40 min at 4°C. The samples were then washed in 0.05 M Na cacodylate for 10 min, followed by

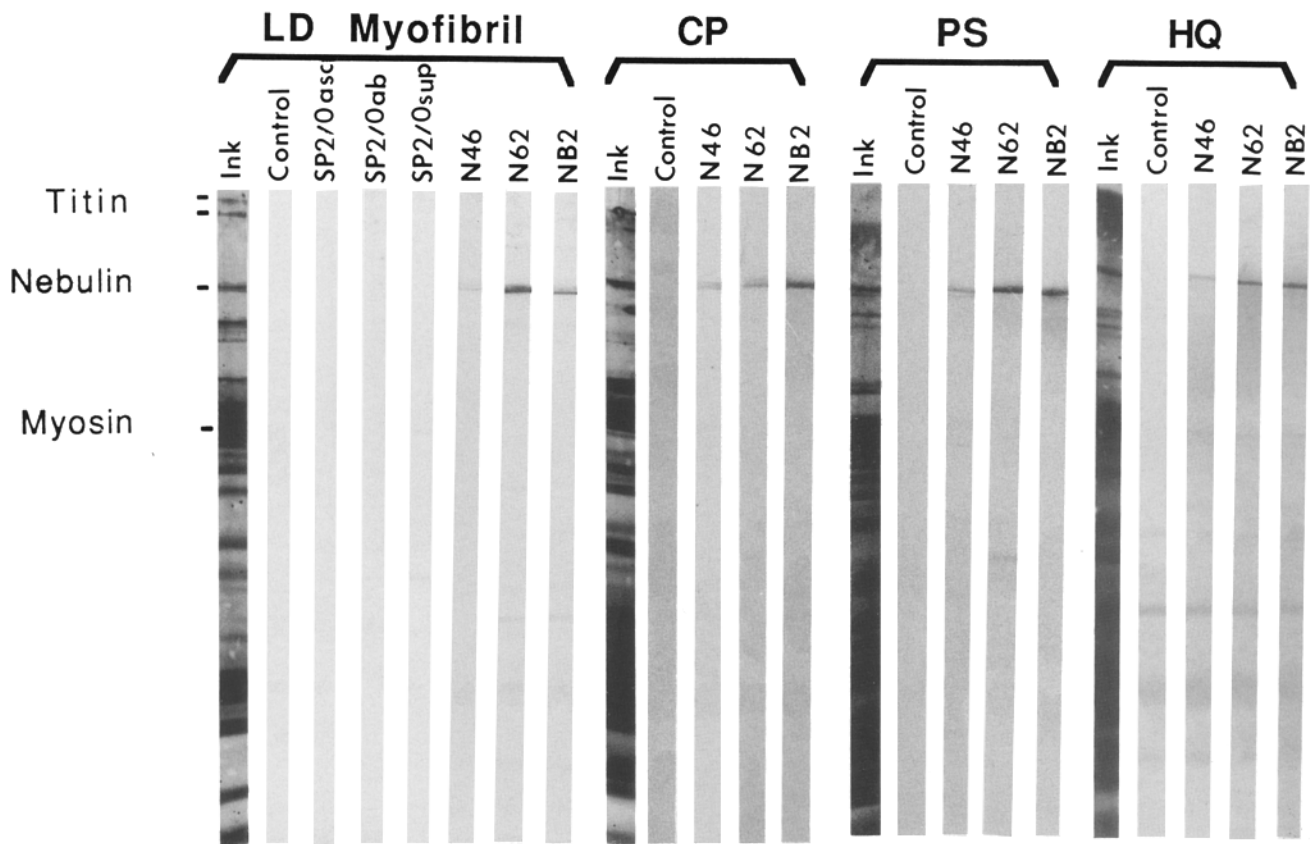


Figure 4. Western blot analysis of three distinct anti-nebulin mAbs. (A) Western blots of total myofibrillar proteins of rabbit longissimus dorsi (LD myofibril) and total tissue proteins of CP, PS, and HQ. All three antibodies (N46, N62, and NB2) recognized nebulin specifically. No labeling was observed in negative controls that either delete mAbs (*control*) or substitute the primary antibodies with ascites (*sp2/0 asc*), supernatant (*sp2/0 sup*), or purified immunoglobulins (*sp2/0 ab*) produced against parent (*sp2/0*) myeloma cells. The low molecular weight bands in HQ samples are nonspecific since they are present in the control sample.

a 20-min water wash just before en bloc staining in 1% aqueous uranyl acetate for 1 h at room temperature. The fibers were washed once in water for 20 min and dehydrated by a graded series of EtOH, two washes in propylene oxide and embedded in Araldyte 506 (a gift from Ciba-Giegy Plastics Division, Hawthorne, NY) prepared by mixing 5 g Araldyte 506, 7.5 g DDSA, 1 g DER 766, 0.25 g DMP-30. Thin sections were cut longitudinally with the edge of a diamond knife (Micro Engineering Inc., Huntsville, TX) parallel to the set of four split fibers. Sections were stained with freshly prepared 1% aqueous potassium permanganate for 20 min followed by Reynold's lead citrate for 5 min, both at room temperature. Micrographs were photographed on a JEOL-100 CX electron microscope. Micrograph magnification was calibrated with a carbon grating standard (No. 1602; Ernest F. Fullam, Inc., Schenectady, NY).

Thin Filament Length Distribution

Thin filament lengths were measured on micrographs from both antibody-labeled muscle fibers and nonlabeled fibers that were fixed and processed directly to access any deleterious effect that prolonged processing might have on thin filament length distribution. For nonlabeled samples, split fibers were mounted on gold slot grids, washed in PBS for 10 min and fixed in 2% glutaraldehyde 0.05 M Na cacodylate, pH 7.4 for 40 min at 4°C. Subsequent processing and embedding were performed as described above for labeled ones. Plastic blocks were trimmed and thick-sectioned sequentially (0.4 μ m) on a Reichert UltraCut E microtome (Reichert Jung, Vienna, Austria) until the phase contrast optical images of stained sections indicated that the four split fibers were in one sectioning plane. Thin sections (80 nm) were then cut and picked up on naked EFFA bar copper grids (No. 22010; Ernest F. Fullam, Inc.) Sections were oriented such that the long axis of the split fibers was roughly perpendicular to the parallel grid bars to ensure that four

fibers could be rapidly screened and photographed with no obstructing bars between the fibers. After staining, the split fiber set was first photographed at a magnification of 250. Each individual fiber was then photographed at 10,000 \times for thin filament length measurements and finally the entire set was rephotographed at 250 \times to complete the session (see Fig. 2). This last step was done to determine the degree of radiation damage. Micrographs of areas with excessive damage were excluded from quantitative measurements. Thin filament length was measured on contact prints from the center of each Z line to the edge of the H zone in overlapping sarcomeres or to the distal end of I-segments in nonoverlapping sarcomeres. Data were tabulated, analyzed (Statview 512⁺; Abacus Concepts, Berkeley, CA), and plotted (Cricket Graph 1.3.2 software; Computer Associates International, San Jose, CA).

Epitope Profiles in Gelsolin-treated Split Fibers

Gelsolin was prepared from human plasma according to Bryan (1) with minor modifications. In our hands, DEAE-purified gelsolin was contaminated with lipoprotein B. Therefore, the preparation was purified further on a Sephacryl S200 column (2.5 \times 50 cm in 800 mM NaCl; 25 mM Tris-Cl; 1 mM EGTA, pH 8.5). Gelsolin was stored at -20°C after adding an equal volume of glycerol. Gelsolin treatment of rabbit psoas split fibers was done as described by Funatsu et al. (3). Briefly, grid-mounted split fibers at rest length, 50 and 100% stretch were treated with 0.5 mg/ml gelsolin in calcium rigor buffer (0.17 M KCl, 10 mM MOPS, 1 mM MgCl₂, 0.1 mM CaCl₂, 2 mM diisopropylfluoride [DFP], and 2 mM leupeptin, pH 7.0) at 4°C for 1 h, and then washed for 30–45 min in the same buffer. The fibers were treated subsequently with 0.5 mg/ml gelsolin in contracting solution (0.15 M KCl, 5 mM MgCl₂, 4 mM ATP, 10 mM MOPS, 0.1 mM CaCl₂, 2 mM DFP, and 2 mM leupeptin, pH 7.0) for 1 h and washed for 1 h in

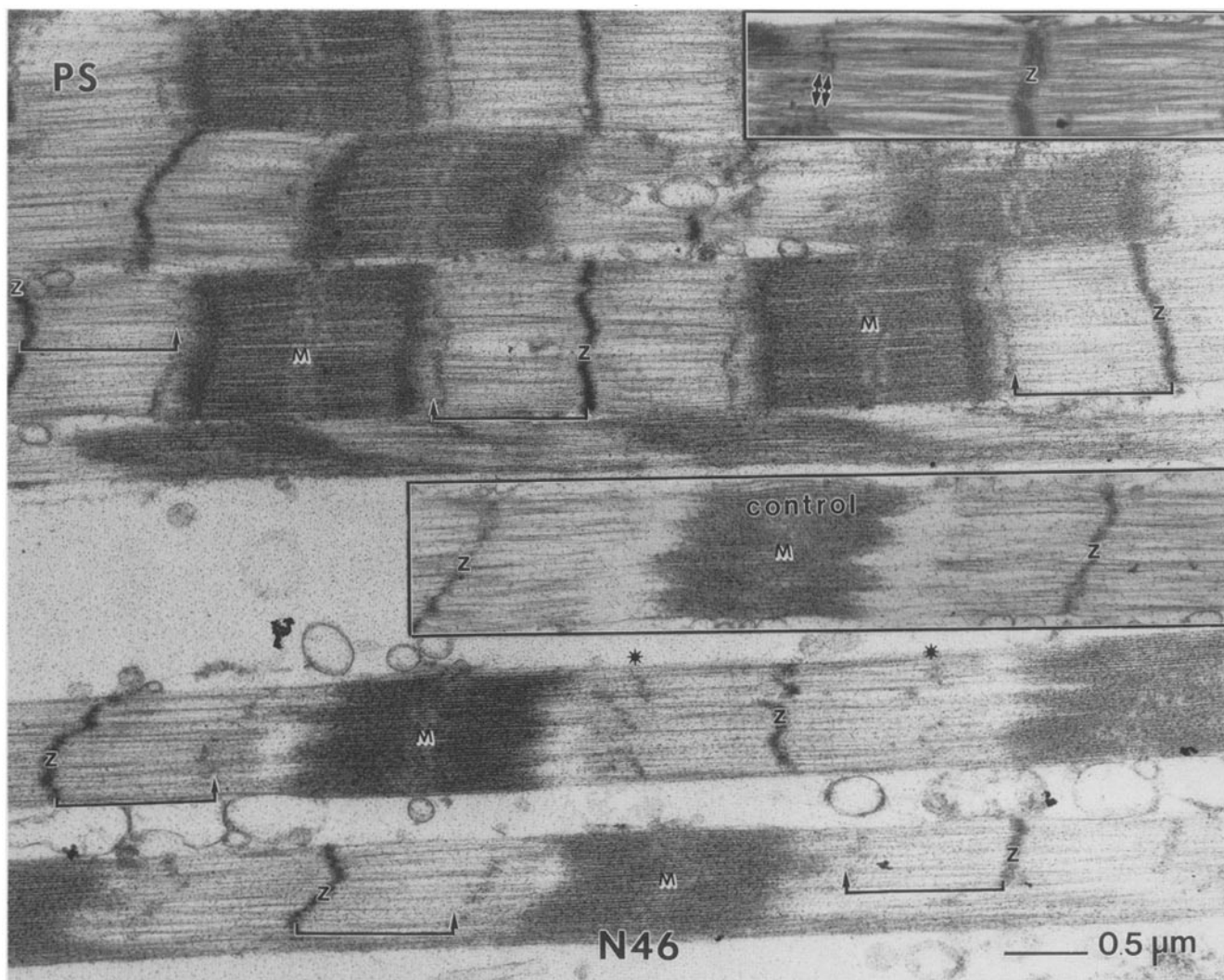


Figure 5. Epitope profiles of monoclonal anti-nebulin N46. Split-fibers of rabbit psoas (PS) skeletal muscle were stretched to various lengths prior to their labeling with N46 and gold-conjugated protein A. Labeled fibers were fixed, embedded in plastic and sectioned. Ascites fluid produced against parent myelomas was used as a negative control (*bottom inset*). N46 labeled a closely spaced doublet (*double arrowheads, top right inset*) per half sarcomere at a constant ($0.85 \mu\text{m}$) distance from the Z line, irrespective of sarcomere length. In long sarcomeres, fragmentation of the Z line led to a parallel change in the contour of the antibody stripe (*asterisks*). Note that the 19th and 20th thin filament repeats correlate with epitope loci (*top inset*).

relaxing solution (0.15 M KCl, 5 mM MgCl₂, 4 mM ATP, 10 mM MOPS, 1 mM EGTA, 2 mM DFP, and 2 mM leupeptin, pH 7.0). The treated fibers were fixed in 3.7% formaldehyde in PBS for 10 min at 0°C and then treated with a mixture of NB2 (1:200 dilution) and N46 (100 μg/ml) for 14 h. Secondary antibody incubation, gold labeling, and electron microscopy were processed as described above.

Results

Nebulin Size Variants and Thin Filament Lengths

To seek a correlation between nebulin size and thin filament length, we investigated a group of six muscles from four species that displayed three size classes of nebulin. Electrophoretic patterns of total muscle proteins (Fig. 1 A) in a gel system optimized for resolving megadalton proteins (23), revealed that nebulin increased in mobility in the following order: human quadriceps (HQ) > snake skeletal (SN) > rabbit psoas (PS) > rabbit longissimus dorsi (LD) > chicken

posterior latissimus dorsi (CPLD) > chicken pectoralis (CP). To estimate their relative molecular weights, muscle samples were mixed with chicken pectoralis (CP) and electrophoresed on a long format gel to enhance mobility differences (Fig. 1 C). Plots of *M*, versus mobility (Fig. 1 D, *inset*), with titin (T1: 2.8×10^6 ; T2: 2.1×10^6), projectin (1.2×10^6), and apolipoprotein B (0.55×10^6) as standards, yielded the following set of values: 890 kD (HQ, SN); 770 kD (LD, PS); 700 kD (CPLD, CP). It should be noted that these values are tentative and are used here to express the 10–30% relative difference in size of nebulin variants, insofar as gel mobility is a measure of size of polypeptides in this range. Their absolute values can vary as much as 15% without affecting the general correlation reached below. That these bands are indeed nebulin was confirmed by immunoblots with anti-nebulin polyclonal antibodies (Fig. 1 B).

Thin filament lengths of five muscles (SN, LD, PS, CPLD, and CP) were determined by electron microscopy. To facili-

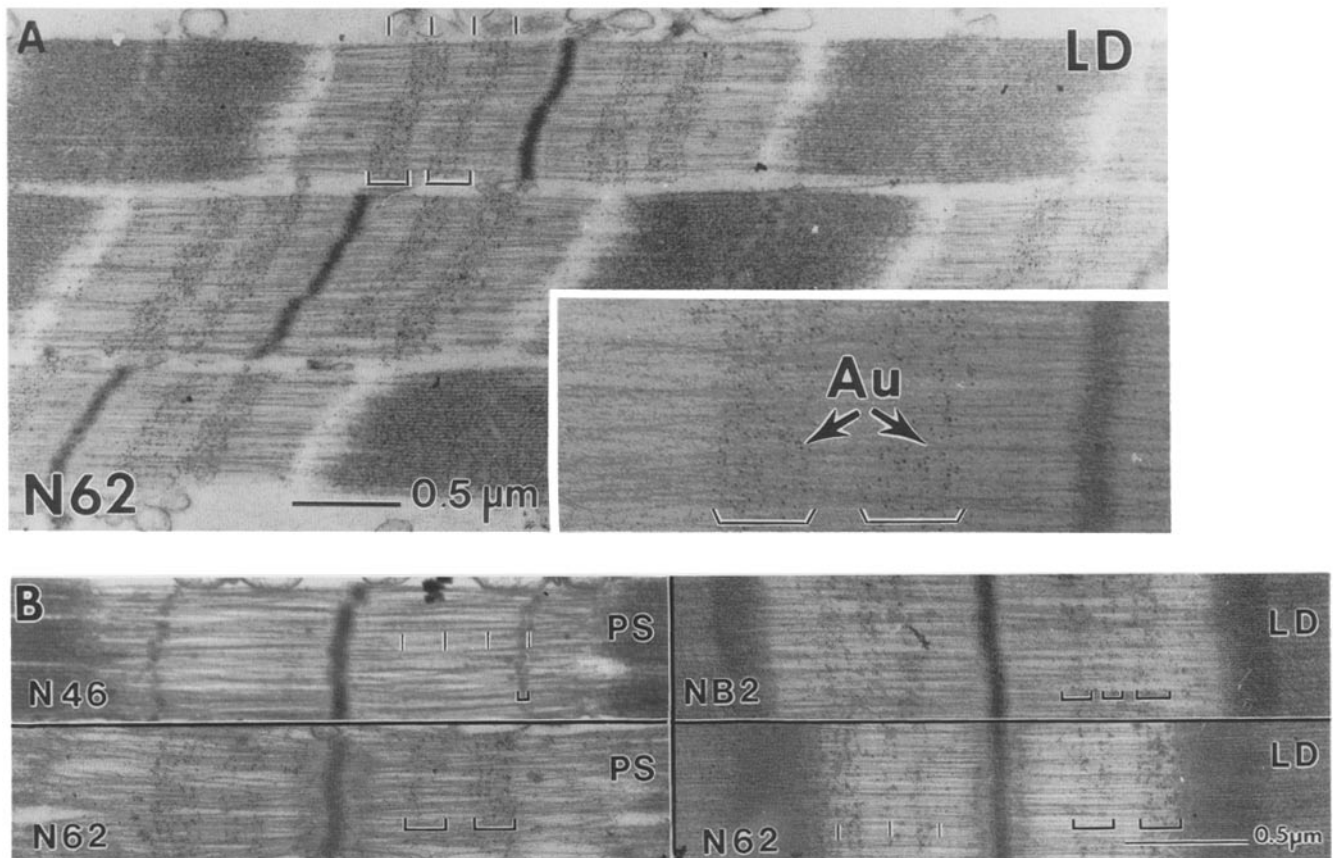


Figure 6. Epitope profiles of N46, N62, NB2, and thin filament periodicity. (A) Epitope profile of N62: N62 labeled a group of 10 stripes spanning from 0.25 to 0.68 μm to the Z line in LD muscle. Note that repetitive epitopes in LD are spaced at 40 nm and its multiples. The higher magnification image (*bottom right inset*) demonstrated specific labeling by gold conjugates (Au). Antibody labeling appears to enhance the intrinsic 40 nm thin filament repeat at these loci (tick marks spacing: 5 repeat). (B) Epitope spacing of N46, N62, and NB2 and thin filament periodicity: NB2 labeled a group of N62 epitopes in LD and in PS. In these selected micrographs, both antibody density and thin filament periodicity are discernable, thus allowing indexing epitope loci on thin filament periodicity. For this purpose, tick marks are provided at every fifth thin filament repeat (N46 in PS, N62 in LD).

tate precise comparison of thin filament lengths and epitope profiles between tissue types, several different fibers were mounted on one grid, processed, sectioned, and photographed as a set (Fig. 2 A). This procedure, although laborious, minimized uncertainties and variations that can occur when muscle fibers are processed individually. Thin filament length, as measured between the center of the Z line to the edge of the H zone of each sarcomere (Fig. 2 B), varied over a narrow range around a characteristic mean value: 1.30 μm for SN; 1.12 μm for PS; 1.13 μm for LD; 1.06 μm for CPLD; and 1.04 μm for CP (Fig. 3). The thin filament length for these five muscles, together with the reported thin filament value (1.35 μm) of human quadriceps skeletal muscle (20), are shown as a function of the relative size of nebulin in each muscle (Fig. 1 D). The plot demonstrated that muscles with longer nebulin have proportionally longer thin filaments. Furthermore, each of the three pairs of muscles with similar size nebulin has similar thin filament length. The positive correlation between the size of nebulin polypeptide and thin filament length in different muscles is consistent with the putative role of nebulin as a coextensive template for actin filaments.

mAbs to Nebulin

Nebulin preparations purified according to our previous procedures (23) were found occasionally to elicit antibodies to titin when injected into mice (our unpublished observation). To remove trace amounts of degraded titin that copurified with nebulin on the S500 gel filtration column, an additional anion-exchange chromatography step was incorporated. The titin-free nebulin preparation was used as an antigen to prepare mAbs. A library of 16 anti-nebulin secreting hybridomas were obtained by fusing spleens of immunized mice with nonsecreting myeloma cells (SP2/0). For the present purpose, we have characterized two distinct antibodies, N46 (IgM) and N62 (IgG₁), from our library, together with NB2 (IgG₁) produced by Furst et al. (4). These mAbs labeled a single band on blots of purified myofibrils from LD and of total muscle proteins of CP, PS, and HQ (Fig. 4). No significant staining was found in negative controls, including those without primary antibody (control), or those with ascites fluids (SP2/0 acs), purified immunoglobulins (SP2/0 ab) produced against parent myeloma cells, or culture supernatant (SP2/0 sup) of parent myeloma cells. Thus these anti-

Antibody	Tissue	Thin Filament Repeat																							
		Z	1	2	3	4	5	6	7	8	9	10	11	12	13	14	15	16	17	18	19	20	21	...	
N46	PS																								
	LD																					+	+		
	CP																					+	+		
N62	PS																								
	LD																								
	CP																								
NB2	PS																								
	LD																								
	CP																								

Figure 7. Summary diagram of epitope index on thin filament repeat. A diagram tabulates the epitope profiles of N46, N62, and NB2 in three muscles (PS, LD, and CP). Plus signs indicate unambiguous assignment. Horizontal lines indicate general epitope loci with uncertain assignment. Due to the composite nature of this diagram, not all loci were observed in all sarcomeres at all times.

bodies are specific for nebulin and distinct epitopes are shared among these muscle tissues and species.

Epitope Profiles of Nebulin Size Variants

These mAbs were used in immunoelectron microscopic studies to map out nebulin organization in the sarcomere and to define differences among size variants. For these purposes, single muscle fibers were split longitudinally and stretched to various lengths before labeling with mAbs. Secondary antibodies and protein A-colloidal gold conjugates were then added to enhance antibody density and detectability. The profiles and stretch behaviors of various nebulin epitopes in sarcomeres from rest length to well over nonoverlap were investigated and the results are shown in Figs. 5, 6, and 8, and summarized in Fig. 7.

N46. As shown in Figs. 5 and 6, N46 gave rise to the simplest epitope profile: A single pair of stripes at 0.85 μm from the center of the Z line in long sarcomeres ($>3.4 \mu\text{m}$) of PS, LD, and CP). In shorter sarcomeres, the labeling was detected as gold clusters on the periphery of the A band at the expected distance from the Z line (data not shown, see reference 23). In highly stretched sarcomeres, the wavy stripes of N46 displayed a similar contour to that of the adjacent Z line (Fig. 5). In favorable images, where the 40-nm thin filament periodicity was discernible, each of the N46 strips appeared as a doublet that coincided with the 19th and the 20th repeats of PS and LD (Fig. 5, top inset, and Fig. 6 B). Labeling in chicken pectoralis was generally fainter (not shown) and might have resulted from a lower affinity of N46 towards the chicken epitope, as suggested by the weaker Western blotting (Fig. 4).

N62. As shown in Fig. 6, A and B, N62 epitope profiles were more complex and consisted of multiple stripes spanning 0.25–0.68 μm from the center of the Z line. The number and loci of epitopes were most clearly displayed in several samples of rabbit LD (Fig. 6 A) and PS (Fig. 6 B) where a moderate degree of antibody labeling allowed the fine structure of the underlying thin filaments to be discerned. Under such conditions, the epitopes were labeled as ten transverse

stripes of fine dots that superimposed on the 40-nm thin filament repeats, which at higher resolutions appeared as clusters of gold beads (Fig. 6 A, inset). The epitope spacing between adjacent stripes of these clusters ranged from 38 to 42

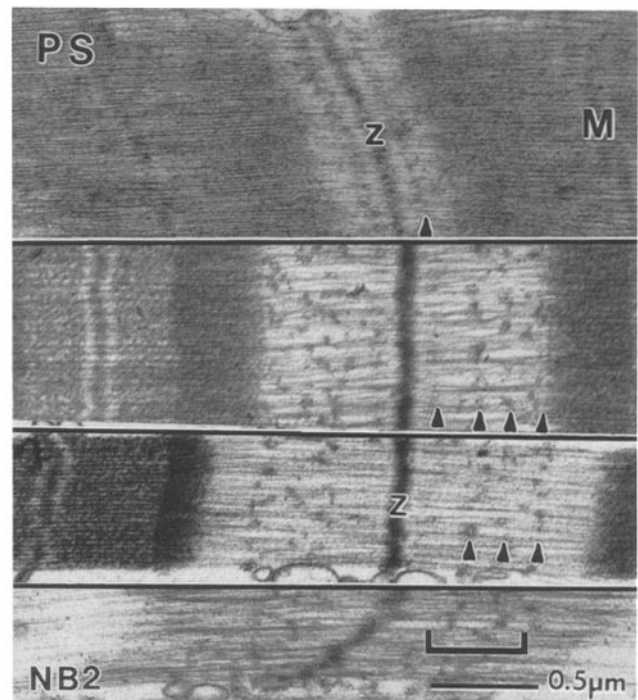


Figure 8. Inextensibility of nebulin upon stretch. Split-fibers of rabbit psoas (PS) skeletal muscle were stretched to various lengths before their labeling with NB2. NB2 labeled four major strips (arrowheads) per half sarcomere in these samples, all at constant distances to the Z line. In shorter sarcomeres, distal stripes entered into the A band and became obscured. Interestingly, labeling of the stripe closest to the Z line seems to intensify in shorter sarcomeres. In nonoverlap sarcomeres (bottom) the stripes were distorted, but remained at fixed loci.

nm and averaged 40 nm. For both muscles, these repetitive epitopes were found at the 6th to 10th, and 13th to 17th thin filament repeats (Fig. 7). For CP, lateral distortion rendered it difficult to discern individual stripes, but the overall distribution of epitopes is similar to those of PS and LD (not shown). A tentative assignment for epitope loci in CP was made and included in Fig. 7.

NB2. As shown in Figs. 6 B and 8, NB2 gave rise to complex epitope profiles consisting of multiple stripes clustered near the central region of thin filaments. For LD (Fig. 6 B) and PS (not shown), three clusters were found, each consisting of two to three stripes of fine dots at identical loci. For CP, two additional stripes were found at the 2nd and 3rd thin filament repeats (not shown).

Epitope Profiles and Sarcomere Length

Over a wide range of sarcomere lengths, epitope profiles of nebulin in PS, LD, and CP muscles are consistent with the notion that nebulin constitutes inextensible longitudinal filaments attached at the Z line. The number of stripes in the I band decreased in shorter sarcomeres as distal epitopes entered the A band. N46 labeled a closely spaced doublet per half sarcomere of PS at a constant ($0.85 \mu\text{m}$) distance from the Z line irrespective of sarcomere length (Fig. 5). In long sarcomeres, fragmentation of the Z line led to a parallel change in the antibody stripe, yet retained the fixed distance to the Z line fragments. NB2, in our hands, gave rise to multiple stripes at fixed sites per half sarcomere in rabbit psoas muscle (Figs. 6 B and 8). Our data thus contrasted those of Furst et al. (4), who reported a single epitope site of NB2 that appeared to have translocated from 0.25 to $0.1 \mu\text{m}$ from the Z line in chicken pectoralis muscle. This discrepancy is yet to be resolved (see Discussion). It is worth noting that other investigators (11, 13) have detected anti-nebulin densities within the overlap zone of A bands when higher antibody concentrations were applied for an extended period of time.

Nebulin in Gelsolin-treated Sarcomeres

To explore the role of actin in the proposed actin–nebulin composite filaments, we applied the gelsolin-treatment of Funatsu et al. (3) to remove thin filaments selectively without extracting nebulin. While applying this technique, we observed that gelsolin frequently removed both actin filaments and the Z line density in rabbit psoas muscles, despite the presence of calpain inhibitor. Antibody staining with a mixture of N46 and NB2 on split psoas fibers that were stretched to various degrees prior to gelsolin treatment revealed that nebulin epitopes were indeed present in the Z line-free sarcomeres. However, labeled epitopes appeared as broad zones, rather than narrow stripes, suggesting lateral misalignment or reorganization of nebulin filaments. In Fig. 9, a pair of $0.33 \mu\text{m}$ wide zones of gold beads was observed in each sarcomere near $3.4 \mu\text{m}$, presumably resulting from staining of NB2 epitopes. In highly stretched sarcomeres ($>4.5 \mu\text{m}$), however, the diffuse epitope zones are 0.7 to $0.9 \mu\text{m}$ wide and greater than the combined width of N46 and NB2 epitopes in nontreated sarcomeres. Such a broadening may occur if nebulin, in the absence of Z-line anchorage and actin association remains inextensible, but becomes attached to titin filaments either through entrapment or by molecular interaction. The possibility that nebulin may aggregate titin

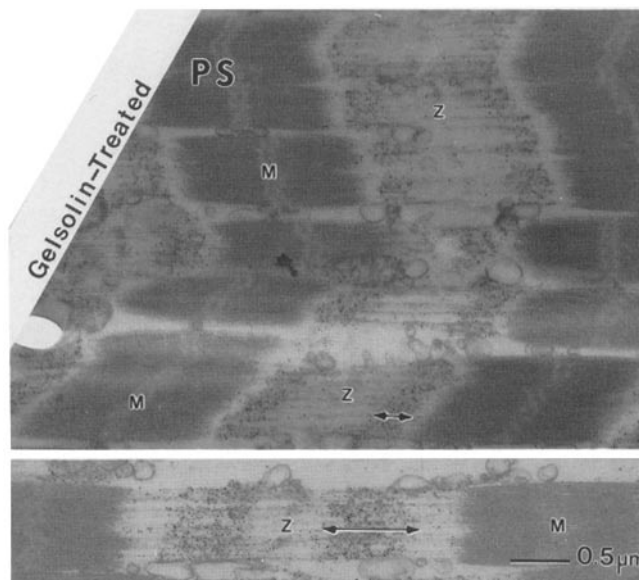


Figure 9. Nebulin epitopes in gelsolin-treated rabbit psoas muscles. Split fibers of rabbit psoas (PS) were stretched to 50 and 100% of rest length and treated with gelsolin to remove thin filaments. The fibers were then fixed and labeled with a mixture of N46 and NB2. Gelsolin treatment frequently removed both actin filaments and the Z line density in rabbit psoas muscle. Nebulin epitopes recognized by N46 and NB2 were no longer aligned laterally in the Z line-free sarcomeres, but were still confined to the general vicinity (top panels). In highly stretched sarcomeres (bottom), however, the epitope zone spanned from 0.7 to $0.9 \mu\text{m}$ (double-headed arrows). Nebulin remained in the sarcomere perhaps by adhering to titin filaments.

filaments in the gelsolin-treated sarcomeres with intact Z lines has been alluded to by Funatsu et al. (3).

Discussion

Architecture of Nebulin Filaments: A Set of Inextensible Molecular Filaments Anchored at the Z Line

Our present immunoelectron microscopic studies of the axial distribution of nebulin epitopes in several skeletal muscles with a panel of mAbs have confirmed and extended earlier observations made with polyclonal anti-nebulin antibodies (11, 13, 23). Since nebulin epitopes maintain constant spacings between epitopes and the Z line over a wide range of sarcomere lengths, these data support our previous proposal that nebulin constitutes a set of longitudinal inextensible filaments anchored at the Z line (23). The data of Furst et al. (4) showing the translocation of a single NB2 epitope toward the Z line in short chicken pectoralis sarcomeres have not been reproduced in our studies that used the same antibody. The discrepancy does not yet have a satisfactory explanation. Whether nebulin extends beyond the distal end of thin filaments is unclear, but no epitopes beyond $1.0 \mu\text{m}$ have yet been detected. The reported labeling of M line by anti-nebulin was suspect due to the questionable specificity of antiserum (as quoted in reference 11). Nebulin may be anchored at the Z line through its interaction with α -actinin (12).

The presence of a unique epitope of N46 at 0.85 μm from the Z line indicates that a single nebulin polypeptide extends at least that far and may well span the entire length of the nebulin filament estimated to be $\sim 1 \mu\text{m}$.

Repetitive Epitopes and Sequence Motifs of Nebulin

The observation that the repetitive epitopes of nebulin are spaced at 40 nm or its multiples suggests that the nebulin polypeptide folds into repetitive domains at such spacings along its length. Since no monoclonal antibodies tested so far labeled every 40-nm repeat throughout the whole length, the sequence or conformation repeats recognized by these antibodies appear to be restricted to certain regions of the molecule. These monoclonal antibodies are thus useful tools in defining the degree of sequence homology and conformational similarity along the nebulin molecule.

In this connection, the 40-nm spacing between repetitive epitopes of N46, N62, and NB2 is significant in exploring the molecular anatomy of nebulin. As presented elsewhere (Wang, K., M. Knipfer, Q. Q. Huang, L. Hsu, A van Heerden, K. Browning, E. Quian, and H. Stedman. 1990. *J. Cell Biol.* 111:428a), our sequence analysis of human nebulin cDNA has demonstrated that the majority of the nebulin protein molecule is composed of a recurring motif of a fundamental 35-residue repeat and a higher order 240-residue repeat containing seven fundamental repeats. An intriguing relationship among these structural parameters exists: if the 35-residue repeat spans a 5–6-nm domain that matches the actin subunit dimension, then the 240-residue repeat would extend 35–40 nm, corresponding to the actin filament periodicity. The entire nebulin molecule of 6,000–8,000 residues would then extend 1,000–1,200 nm, matching the length of the thin filaments. We proposed that a simple scaling factor between polypeptide size and protein contour length would allow nebulin to act as an actin filament template by domain matching with actin subunits.

The present studies indicate that a 40-nm nebulin repeating domain does indeed exist in the sarcomere. Whether or not the 40-nm repeating domain corresponds to the 240-residue sequence repeat awaits protein sequence analysis of these epitopes.

Epitope Profiles of Nebulin Variants

The epitope profiles of nebulin variants are strikingly similar, indicating that their molecular structures are highly conserved, at least in the regions probed by this panel of monoclonal antibodies. These data suggest that the extra protein segments in nebulin variants are probably located at either or both ends of these molecules. Since epitope profiles reflect the folding patterns of native proteins, the extensive similarity suggests that the contour length of native nebulin is proportional to its polypeptide size. It follows that the correlation between thin filament length and nebulin polypeptide size can be extended to thin filament length and native nebulin length.

Nebulin as a Length-regulating Template Protein: Coextensiveness of Nebulin and Thin Filaments

An intimate association between nebulin and the thin filament is suggested by the following features of anti-nebulin-labeled sarcomeres: first, nebulin epitopes labeled discrete

loci on thin filaments; second, the epitope loci, when clearly resolved, indexed on the underlying thin filament repeats. These images may be accounted for if nebulin molecules lay alongside actin filaments and interact with the latter by matching nebulin domain repeats with actin helical repeats. The data, taken together with the stoichiometry of 2 to 4 of nebulin polypeptides per actin filament (23), support a molecular template role for nebulin in the construction of a nebulin-actin composite filament. This molecular template acts as a protein ruler by matching its large number of 40-nm repeating domains with an equal number of helical repeats of actin filaments. Whether nebulin domains contribute significantly to the distinct electron densities of thin filament repeats in unlabeled sarcomeres, which are commonly attributed to troponin complexes, remains open.

The protein ruler hypothesis received further support by the positive correlation between the size of nebulin polypeptides and the length of thin filaments in a group of six skeletal muscles. Since the contour length of nebulin is likely to be proportional to polypeptide size, the simplest and most intriguing interpretation of this correlation is that the thin filament length is equal to the contour length of the nebulin molecule. It was noted previously (23) that thin filament length varies widely from 0.4 to 1.6 μm in the cardiac sarcomere (15, see also reference 19). This pronounced length heterogeneity may have resulted from the complete absence of nebulin to guide assembly (23).

Taken together, current data support that nebulin is necessary to provide uniform length distributions of thin filaments within each sarcomere, but is not required for thin filament assembly. Whether these nebulin variants also serve tissue-specific functions of the thin filaments remains to be explored.

Nebulin as a Molecular Filament of a Three-dimensional Sarcomere Matrix

The overall three-dimensional architecture of the sarcomere matrix, especially the inter-connectivity of titin and nebulin filaments, is yet unclear. Funatsu et al. (3) reported possible branching of elastic filaments in gelsolin-treated sarcomeres, but did not distinguish the individual contributions of titin and nebulin to the filamentous structure. Our studies suggest that nebulin, when released of its anchorage to the Z line and its association to actin in gelsolin-treated sarcomeres, most likely remained inextensible, albeit translocated longitudinally (Fig. 9). Since excessive stretch caused nebulin to lose lateral registration, the data support the existence of direct or indirect structural linkages of dislodged nebulin to titin filaments in gelsolin-treated sarcomeres. These interactions, if they exist in intact sarcomeres, are likely to be liable because titin and nebulin display distinct stretch responses that preclude a stable association between the two in the presence of the actin filament (see 10, 21, 22 for reviews).

The structural model that has emerged from our recent studies of titin and nebulin depicts the "thick" filament as a composite filament of myosin and titin and the "thin" filament as a composite filament of actin and nebulin (23). The two giant molecules share the unique architectural feature in that each molecule is a full-length template. The covalent nature of these molecules is ideally suited as a template to direct the self-assembly of smaller building blocks into repetitive structures of uniform length, since instructions for assembly

are directly and covalently encoded in a linear fashion in the protein domains and the gene sequence of the template molecule. Molecular templates thus confer uniformity in the assembly of thick and thin filaments.

We thank G. Gutierrez and R. Borden for expert assistance in nebulin purification and Western blots and P. Hoops and P. D. Gottlieb of the Hybridoma Facilities of the University of Texas for assistance in hybridoma production.

This work was supported in part by National Institutes of Health grant DK 20270 and a grant from the Foundation for Research (to K. Wang). M. Kruger gratefully acknowledges the support of a Postdoctoral Fellowship from the Foundation for Research Development (South Africa).

Received for publication 2 January 1991 and in revised form 10 May 1991.

References

1. Bryan, J. 1988. Gelsolin has three actin-binding sites. *J. Cell Biol.* 106:1553-1562.
2. Davis, J. S. 1988. Assembly processes in vertebrate skeletal thick filament formation. *Annu. Rev. Biophys. Biophys. Chem.* 17:217-239.
3. Funatsu, T., H. Higuchi, and S. Ishiwata. 1990. Elastic filaments in skeletal muscle revealed by selective removal of thin filaments with plasma gelsolin. *J. Cell Biol.* 110:53-62.
4. Furst, D., M. Osborn, R. Nave, and K. Weber. 1988. The organization of titin filaments in the half sarcomere revealed by monoclonal antibodies in immunoelectron microscopy: a map of ten non-repetitive epitopes starting at the Z line extends close to the M line. *J. Cell Biol.* 106:1563-1572.
5. Hu, D. H., S. Kimura, and K. Maruyama. 1986. Sodium dodecyl sulfate gel electrophoretic studies of connectin-like high molecular weight proteins of various types of vertebrate and invertebrate muscle. *J. Biochem. (Tokyo.)* 99:1485-1492.
6. Hu, D. H., A. Matsuno, K. Terakado, T. Matsuura, L. Kimura, and K. Maruyama. 1990. Projectin is an invertebrate connectin (titin): isolation from crayfish claw muscle and localization in crayfish claw muscle and insect flight muscle. *J. Muscle Res. Cell Motil.* 11:497-511.
7. Jin, J.-P., and K. Wang. 1991. Nebulin as a giant actin-binding template protein in skeletal muscle sarcomere: interaction of actin cloned human nebulin fragments. *FEBS (Fed. Eur. Biochem. Soc.) Lett.* 281:93-96.
8. Kyhse-Anderson, J. 1984. Electroblotting of multiple gels: a simple apparatus without buffer tank for rapid transfer of proteins from polyacrylamide to nitrocellulose. *J. Biochem. Biophys. Methods.* 10:203-209.
9. Locker, R. H., and D. J. C. Wild. 1986. A comparative study of high molecular weight proteins in various types of muscle across the animal kingdom. *J. Biochem. (Tokyo.)* 99:1473-1484.
10. Maruyama, K. 1981. Connectin, an elastic filamentous protein of striated muscle. *Int. Rev. Cytol.* 104:81-114.
11. Maruyama, K., A. Matsuno, H. Higuchi, S. Shimaoka, S. Kimura, and T. Shimizu. 1989. Behavior of connectin (titin) and nebulin in skinned muscle fibers released after extreme stretch as revealed by immunoelectron microscopy. *J. Muscle Res. Cell Motil.* 10:350-359.
12. Nave, R., D. O. Furst, and K. Weber. 1990. Interaction of α -actinin and nebulin in vitro. Support for the existence of a fourth filament system in skeletal muscle. *FEBS (Fed. Eur. Biochem. Soc.) Lett.* 269:163-166.
13. Pierobon-Bormioli, S., R. Betto, and G. Salviati. 1989. The organization of titin and nebulin in the sarcomeres: an immunolocalization study. *J. Muscle Res. Cell Motil.* 10:446-456.
14. Pollard, T. D., and J. A. Cooper. 1986. Actin and actin-binding proteins. A critical evaluation of mechanisms and functions. *Annu. Rev. Biochem.* 55:987-1036.
15. Robinson, T. F., and S. Winegrad. 1977. Variation of thin filament length in heart muscle. *Nature (Lond.)* 267:74-75.
16. Somerville, L., and K. Wang. 1981. The ultrasensitive silver protein stain also detects nanograms of nucleic acids. *Biochem. Biophys. Res. Commun.* 102:52-58.
17. Stossel, T. P., C. Chaponnier, R. M. Ezzell, J. H. Hartwig, P. A. Janmey, D. J. Kwiatkowski, S. E. Lind, D. B. Smith, F. S. Southwick, H. L. Yin, and K. S. Zaner. 1985. Nonmuscle actin-binding proteins. *Annu. Rev. Cell Biol.* 1:353-402.
18. Swerdlow, P. S., D. F. Finley, and A. Varshavsky. 1986. Enhancement of immunoblot sensitivity by heating of hydrated filters. *Anal. Biochem.* 156:147-153.
19. Traeger, L., and M. A. Goldstein. 1983. Thin filaments are not of uniform length in rat skeletal muscle. *J. Cell Biol.* 96:100-103.
20. Walker, M. S., and G. A. Schrodt. 1974. I segment lengths and thin filament periods in skeletal muscle fibers of the Rhesus monkey and human. *Anat. Rec.* 178:63-82.
21. Wang, K. 1985. Sarcomere-associated cytoskeletal lattices in striated muscle. *Cell Muscle Motil.* 6:315-369.
22. Deleted in proof.
23. Wang, K., and J. Wright. 1988. Architecture of the sarcomere matrix of skeletal muscle: Immunoelectron microscopic evidence that suggests a set of parallel inextensible nebulin filaments anchored at the Z line. *J. Cell Biol.* 107:2199-2212.